Journal of NeuroVirology, 15: 139–152, 2009

ISSN 1355-0284 print / 1538-2443 online
DOI: 10.1080/13550280802534763

informa
healthcare

Dual lentivirus infection potentiates neuroinflammation and neurodegeneration: viral copassage enhances neurovirulence

Amir Afkhami-Goli,[1,2] Shu-Hong Liu,[3] Yu Zhu,[1] Joseph M Antony,[1] Hosseinali Arab,[2] and Christopher Power[1,3]

[1]Departments of Medicine and Medical Microbiology and Immunology, University of Alberta, Edmonton, Alberta, Canada; [2]Department of Pharmacology, Faculty of Veterinary Medicine, University of Tehran, Tehran, Iran; and [3]Department of Clinical Neurosciences, University of Calgary, Calgary, Alberta, Canada

Infection by multiple lentiviral strains is recognized as a major driving force in the human immunodeficiency virus/acquired immunodeficiency syndrome (HIV/AIDS) epidemic, but the neuropathogenic consequences of multivirus infections remain uncertain. Herein, we investigated the neurovirulence and underlying mechanisms of dual lentivirus infections with distinct viral strains. Experimental feline immunodeficiency virus (FIV) infections were performed using cultured cells and an *in vivo* model of AIDS neuropathogenesis. Dual infections were comprised of two FIV strains (FIV-Ch and FIV-PPR) as copassaged or superinfected viruses, with subsequent outcome analyses of host immune responses, viral load, neuropathological features, and neurobehavioral performance. Dual infections of feline macrophages resulted in greater *IL-1β* (interleukin-1β), *TNF-α* (tumor necrosis factor α), and *IDO* (indoleamine 2,3-dioxygenase) expression and associated neurotoxic properties. FIV coinfection and sequential superinfection *in vivo* also induced greater *IL-1β*, *TNF-α,* and *IDO* expression in the basal ganglia (BG) and cortex (CTX), compared to the monovirus- and mock-infected groups, although viral loads were similar in single virus– and dual virus–infected animals. Immunoblot analyses disclosed lower synaptophysin immunoreactivity in the CTX resulting from FIV super- and coinfections. Cholinergic and GABAergic neuronal injury was evident in the CTX of animals with dual FIV infections. With increased glial activation and neuronal loss in dual FIV–infected brains, immunohistochemical analysis also revealed elevated detection of cleaved caspase-3 in dysmorphic neurons, which was associated with worsened neurobehavioral abnormalities among animals infected with the copassaged viruses. Dual lentivirus infections caused an escalation in neuroinflammation and ensuing neurodegeneration, underscoring the contribution of infection by multiple viruses to neuropathogenesis. *Journal of NeuroVirology* (2009) **15,** 139–152.

Keywords: FIV; nervous system; dual infection; neuroinflammation; neuron; glia; apoptosis

Address correspondence to Dr. Christopher Power, Department of Medicine (Neurology), 611 HMRC, University of Alberta, Edmonton, AB, T6G 2S2 Canada. E-mail: chris.power@ualberta.ca

Amir Afkhami-Goli and Shu-Hong Liu contributed equally to this study.

These studies were supported by the Canadian Institutes of Health Research (CIHR). A.A.-G. was supported by a scholarship from the Iranian Ministry of Science. J.M.A. was supported by a Studentship from the Multiple Sclerosis Society of Canada. Y.Z. holds a Fellowship from the CIHR. C.P. holds a Canada Research Chair (Tier 1) in Neurological Infection and Immunity and is an Alberta Heritage Medical Research Senior Scholar. The authors thank Martine Ooms and Neda Shariat for technical assistance and Stephanie Skinner and Leah DeBlock for manuscript preparation.

Received 26 June 2008; revised 18 August 2008; accepted 7 October 2008

Introduction

Infection by multiple strains of human immunodeficiency virus type 1 (HIV-1) represents an important source of viral diversity in the current HIV/AIDS (acquired immunodeficiency syndrome) epidemic (Taylor *et al,* 2008). Indeed, several of the principal HIV-1 strains identified globally are derived from recombination between different primary strains, which present major challenges in terms of developing vaccines (Klausner *et al*, 2003) and implementing antiretroviral therapies (Kantor and Katzenstein, 2004). A hallmark of all pathogenic lentivirus infections is extensive viral genetic diversity as a consequence of the error-prone nature of the viral reverse transcriptase (RTase) and a propensity for viral recombination, coupled with high rates of virion production that are modulated by immune selection (Patrick *et al*, 2002). The pivotal step in retroviral recombination is the simultaneous infection by two or more viral strains of the same cell during a single transmission event (coinfection) or through sequential viral infection during multiple transmission events (superinfection). To date, much of the knowledge about dual retroviral infections is derived from *ex vivo* studies (Kim *et al,* 1993, 1996), clinical case reports documenting dual infection with HIV-1 and HIV-2 (Andersson *et al*, 1999; Sarr *et al*, 2000) or by examining viruses belonging to different HIV-1 subtypes as superinfections (Fang *et al*, 2004; Takehisa *et al*, 1997) or coinfections (Iversen *et al*, 1999; Ramos *et al*, 1999; Becker-Pergola *et al*, 2000; Long *et al*, 2000; Thomson *et al*, 2001). Indeed, there is compelling evidence that both drug-sensitive and -resistant HIV-1 strains exist concurrently in infected individuals and each strain predominates depending on the antiretroviral regimen efficacy (Brumme and Harrigan, 2006). While bearing viral interference in mind and the fact that, at least in the case of superinfections, the primary viral infection may result in subsequent resistance to the latter infection(s) (reviewed in Nethe *et al*, 2005), there is no widespread consensus regarding the real prevalence of dual HIV strain infection, although the widespread detection of circulating recombinant form (CRFs) is compelling evidence that dual infection occurs (Takeb *et al*, 2004).

Feline immunodeficiency virus (FIV) is a member of the lentivirus subfamily; it causes persistent infection in domestic cats and shares many of the immunological and neurological properties with HIV (Bendinelli *et al*, 1995). FIV causes neurological disorders in 20% to 40% of naturally infected cats by entering the nervous system and infecting parenchymal microglia, perivascular macrophages, and astrocytes (Power, 2001). Neuropathogenic effects mediated by FIV infection are viral strain specific (Power *et al*, 1998; Johnston *et al*, 2002b) and range from impaired motor activity, seizures, as well as behavioral abnormalities such as psychomotor slowing, aggressiveness, disrupted sleep and arousal patterns (Phillips *et al*, 1994; Prospero-Garcia *et al*, 1999). Neuroimmune activation during FIV infection is accompanied by neuronal injury in the basal ganglia and cortical regions. Indeed, microglial and astroglial activation are cardinal features of FIV infection, although multinucleated giant cells are rarely observed in FIV infection (Power *et al*, 1997; Noorbakhsh *et al*, 2006).

Although dual lentiviral infections occur *in vivo* (Blackard *et al*, 2002), the neurologic consequences of dual infection in terms of viral properties such as neurotropism, replication kinetics, neuroimmune responses, and ensuing disease progression have not been fully investigated. Previous studies of HIV-1 have focused on a blood-derived evidence of dual lentivirus infection, reflecting largely T-cell infection. However, the extent of dual infection of monocytoid cells, which are the principal target cells in the brain, is unknown. Dual HIV-1 infection of brain is apparent from several reports (Smit *et al*, 2004), with evidence of viral recombination (Zhang *et al*, 2001) and an association with HIV-associated dementia (Salemi *et al*, 2005). We hypothesized that dual lentivirus infection with two distinct neurovirulent lentivirus strains would worsen neurologic disease by amplifying the underlying pathogenic mechanisms. The present studies indicated that infection by two FIV strains, known to cause neurologic disease, resulted in enhanced neuroinflammation and neurodegeneration, which was dependent on the specific infection paradigm.

Results

Dual infection with FIV-Ch and FIV-PPR

The sensitivity of the FIV *pol* primers was assessed by amplifying 10-fold serial dilutions of FIV-Ch and FIV-PPR plasmid added to equal amounts of healthy (uninfected) feline peripheral blood mononuclear cell (PBMC)-derived cDNA (Figure 1A). To determine if both FIV-Ch and FIV-PPR were detected in dual-infected primary feline monocyte-derived macrophage (MDM) cultures, we digested the polymerase chain reaction (PCR) amplicons for FIV-Ch and FIV-PPR *pol* with *Dra* I, revealing different digestion patterns with a 214-bp undigested band for FIV-Ch but 120- and 94-bp digested bands for FIV-PPR. Indeed, different restriction digestion patterns of *pol* amplicons obtained from FIV-infected MDMs showed that each viral strain was detectable. In MDMs superinfected simultaneously with both viruses (FIV-SI) or infected with copassaged viruses (FIV-CP), at day 3 (data not shown) and day 6 post infection (p.i.) (Figure 1B) amplicons corresponding to both FIV strains were evident. These studies indicated that both viruses were present in MDMs

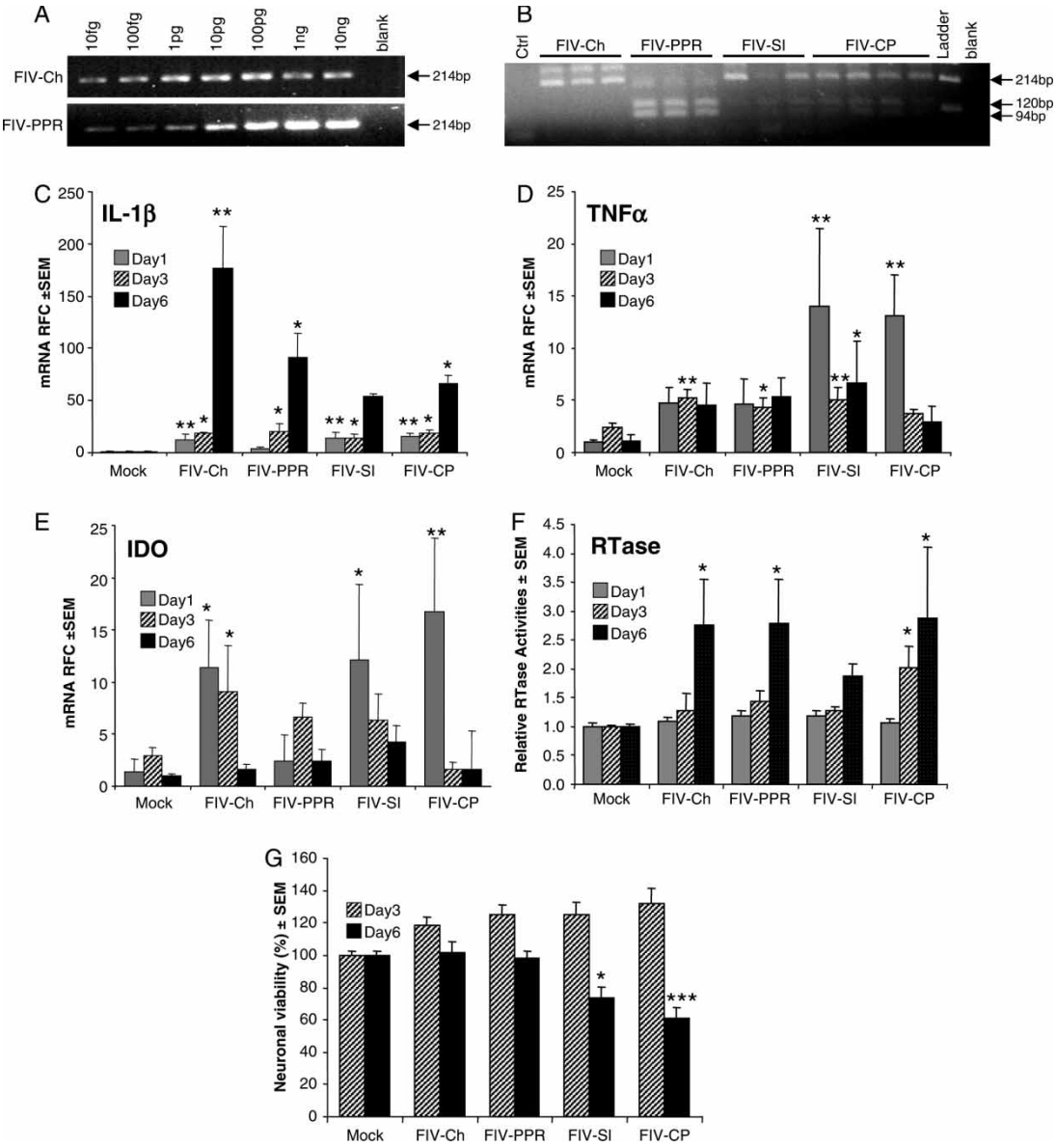

Figure 1 Detection of viral genome and replication in monocytoid cells. (**A**) Viral detection was performed by amplifying 10-fold serial dilutions of FIV-Ch or -PPR provirus with *pol* set 1 primers. (**B**) Differential restriction digestion of the FIV *pol* amplicon derived from MDMs infected with FIV-Ch or FIV-PPR viral strains was observed for each viral strain but superinfected (FIV-SI) and copassaged (FIV-CP) virus–infected MDMs showed both restriction patterns, at day 6 post infection (p.i.). (**C–E**) Real-time RT-PCR analysis revealed mRNA levels (expressed as relative fold change [RFC]) of (**C**) *IL-1β*, (**D**) *TNF-α*, and (**E**) *IDO* after infection of feline MDMs with individual viral strains, FIV-Ch or FIV-PPR, FIV-SI or FIV-CP, at days 1, 3, and 6 p.i. (**F**) Reverse transcriptase (RTase) activity confirmed virus production in MDM supernatants and revealed an increase in RTase at day 6 p.i. in all infected groups, although there was also greater virus production at day 3 p.i. in the FIV-CP–infected cultures. (**G**) Neurotoxic properties of MDM supernatants at day 3 and 6 p.i. were assessed by measurement of βIII-tubulin immunoreactivity (presented as percentage cell viability relative to the mock group). Supernatants from both dual FIV-infected macrophages were toxic to human neurons (LAN-2) at day 6 p.i., whereas this toxicity was significantly higher in supernatants from FIV-CP–infected macrophages. (Data are presented as mean ± SEM; Dunnet's *post hoc* test, $*P < .05$; $**P < .01$; $***P < .001$; $n \geq 3$ MDM donors.)

after infection and they could be distinguished based on the restriction fragment length polymorphism (RFLP) analysis.

To assess the inflammatory features of dual FIV infection in macrophages, we analyzed the transcript levels of the proinflammatory mediators, interleukin (IL)-1β, tumor necrosis factor (TNF)-α, and indoleamine 2,3-dioxygenase (IDO) at different time points after infection. Reverse transcriptase (RT)-PCR analysis revealed a robust and continuous increase in *IL-1β* mRNA levels at day 1 p.i. and thereafter in all infected groups, except for FIV-PPR cultures (Figure 1C). *TNF-α* levels were also upregulated by FIV monoinfections, whereas dual infections further escalated induction at day 1 p.i. (Figure 1D). Of interest, FIV-Ch–infected MDMs

showed an up-regulation of *IDO*, which was also up-regulated in both FIV dual-infected MDM cultures at day 1 p.i. (Figure 1E). Virus production in MDMs was assessed by reverse transcriptase (RTase) activity in culture supernatants, revealing an increase at day 6 p.i. in all groups, although there was also more virus production at day 3 p.i. in FIV-CP–infected cells (Figure 1F). These data indicated that both FIV strains could be detected using the present PCR protocol, whereas dual FIV infections had limited effect on overall viral production. To explore the neurotoxic consequences of FIV-induced immune activation, neurons were incubated with MDM-derived supernatants with or without prior FIV infection. These studies disclosed that supernatants from MDMs coinfected with both FIV strains at day 6 p.i. were toxic to neurons, although supernatants from macrophages infected with FIV-CP showed relatively greater neurotoxic properties (Figure 1G). The present analyses suggested that dual infection exerted variable effects on host immune responses, although overall viral replication was not substantially affected by dual infection. However, dual infection was more neurotoxic, particularly for the copassaged virus paradigm.

Analyses of viral load and CD4$^+$ and CD8$^+$ T-cell levels

To compare the relative abundance of FIV genome in different tissue compartments, we measured viral RNA levels, which revealed similar levels of FIV *pol* transcripts (approximately 3 $\log_{10}$ copies/μg RNA among all FIV-infected groups) in both cerebrospinal fluid (CSF) (Figure 2A) and plasma (data not shown). Semiquantitative (S-Q) real-time RT-PCR revealed no significant differences in FIV *pol* transcript levels in the basal ganglion (BG) and cortex (CTX) among all FIV-infected groups (Figure 2B). Likewise, quantitative analyses also revealed that viral load was similar in the brains of FIV-infected groups (approximately 2 $\log_{10}$ copies/μg RNA), regardless of infection paradigm (Figure 2C). Analyses of FIV *pol* RNA sequences by restriction digestion after amplification revealed that FIV-Ch and FIV-PPR monovirus infections were present in the brain (Figure 2D), depending on the infection paradigm. However, the presence of both viruses was evident only in the brains of animals infected with the copassaged viruses (Figure 2D). Assessment of T-lymphocyte counts in blood revealed a rise in CD4$^+$ T-cell levels in the mock-infected group between weeks 8 and 12 p.i., unlike FIV-infected groups, which showed no change or some suppression at 8 and 12 weeks p.i. in copassaged virus–infected cats. CD8$^+$ T-cell levels showed no change between 8 and 12 weeks in the mock-infected group, but were housed and handled according the FIV-PPR lymphocyte levels were not available. The FIV-Ch and FIV-SI groups showed a modest increase, whereas the FIV-CP group showed higher CD8$^+$ levels at week 8 p.i., followed by suppression. In this short period of *in vivo* infection, dual infection did not demonstrate substantial differences in terms of viral load or immunosuppression compared to matched monovirus infections.

Neuroimmune responses to FIV infection

To assess the neuroinflammatory aspects of dual FIV infection, we investigated the transcript levels of inflammatory genes in the different brain regions. We initially examined the expression of *CXCR4* because it is a principal receptor for FIV, which disclosed reduced transcript levels in all FIV-infected groups (Figure 3A) but this diminished expression was significant in only the FIV-PPR group for both the basal ganglia and cortex. FIV infection induced the expression of *IL-1β* in CTX, of all groups, albeit nonsignificantly (Figure 3B). *TNF-α* expression was up-regulated, in the BG in the FIV dual infection groups, compared to noninfected animals (Figure 3C). However, FIV dual infections markedly induced up-regulation of *IDO* in both brain regions, but this was significant for this enzyme in only the brains of animals infected with FIV-CP (Figure 3D). These studies implied that dual infection induced inflammatory gene expression in the brain and the copassaged viruses exerted a particularly robust effect on *IDO* expression.

Regional neuronal injury

Neuronal degeneration is a pivotal feature of lentivirus neuropathogenesis. Using semiquantitative Western blot analyses to explore differential neuronal injury in brain regions of FIV-infected cats, we examined protein levels of specific neuronal markers, including synaptophysin, vesicular acetylcholine transferase, and glutamate dearboxylase$_{65/67}$, in BG and CTX of FIV-infected cats (Figure 4A). Immunoreactivity of the synaptic marker, synaptophysin, showed no differences in the BG among all groups, unlike the CTX, in which both dual infection groups displayed reduced synaptophysin protein levels, particularly in animals infected with FIV-CP (Figure 4B). We next examined the protein levels of the cholinergic neuronal marker, vesicular acetylcholine transferase (VAChT), and the GABAergic neuronal marker, GAD$_{65/67}$. Similar to synaptophysin, there was no significant change in VAChT (Figure 4C) or GAD$_{65/67}$ (Figure 4D) immunoreactivity levels in the BG among all groups. In the CTX, both dual infection groups showed reduced expression of these neuronal proteins. Of note, monoinfection with FIV-Ch also suppressed both neuronal proteins in the CTX, in keeping with earlier studies of cerebral injury in FIV infection (Johnston *et al*, 2002a). In parallel with immunohistochemical

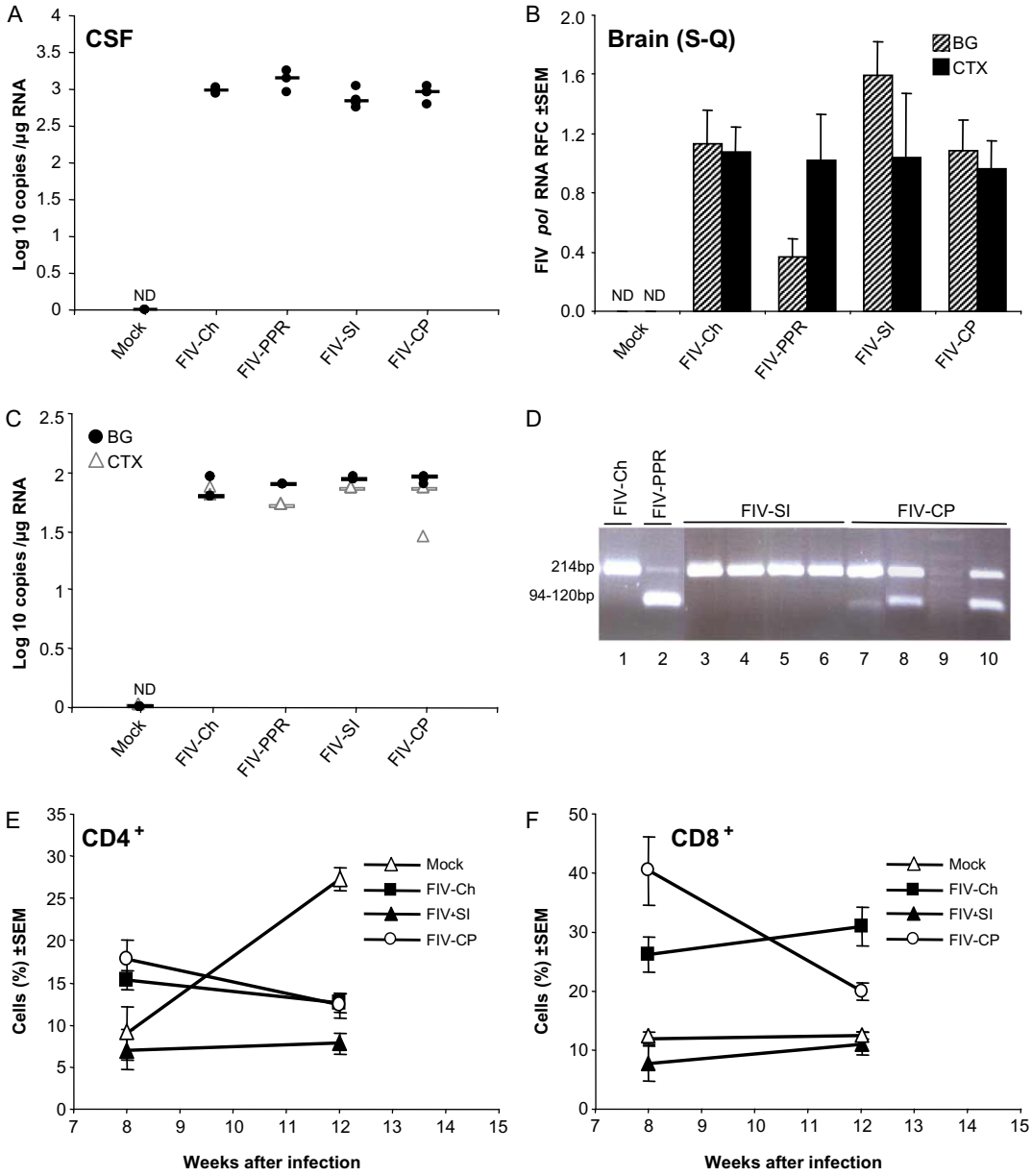

Figure 2 FIV viral load and $CD4^+/CD8^+$ T cell levels. (**A**) Quantitative real-time RT-PCR analysis using primers that detect both FIV-Ch and -PPR disclosed similar levels of FIV *pol* gene transcripts in CSF along all FIV-infected groups. (**B**) Semiquantitative (SQ) real-time RT-PCR analysis shows no significant difference in RNA levels of FIV *pol* gene in basal ganglion (BG) and cortex (CTX) between all FIV-infected cat brains. Quantitative analysis also confirmed the similar levels of brain viral load in BG and CTX (**C**) among all FIV-infected groups. Restriction digestion of viral *pol* PCR amplicon using brain-derived cDNA revealed the presence of each viral strain in monoinfected animals, but only FIV-Ch *pol* was detected in FIV-SI animals, whereas animals receiving FIV-CP showed genomes for both viruses (lanes 1 and 2, monovirus infections; lanes 3 to 6, FIV-SI; lanes 7, 8, 10, FIV-SP; lane 9, DNA ladder) (**D**). (**E**) Assessment of $CD4^+$ T-cell levels in blood showed a rise in levels in the mock-infected group between 8 and 12 weeks p.i., unlike the FIV-Ch, FIV-SI, and FIV-CP groups. (**F**) $CD8^+$ T-cell counts were not altered between 8 and 12 weeks in mock-infected group, but slightly increased in FIV-Ch or FIV-SI groups, whereas FIV-CP–infected cats had relatively higher levels of $CD8^+$ T lymphocytes at 8 weeks p.i., followed by significant suppression up to 12 weeks p.i. The oligonucleotide primers: (*pol* set 1) forward primer: 5′-ACC TAC TTC TAG AGA AGC CTG G-3′; reverse primer: 5′-GTA TCT GTC CAA TAG GCT GC-3′, recognizing both PPR and Petaluma *pol* gene, were used to yield a 214–base pair product. (ND, nondetectable; — represents median; $n \geq 4$ animals per group.)

studies, both brain regions exhibited lower levels of neuronal nuclei protein (NeuN) immunoreactivity in all infected groups, which was statistically significant only in the cortices of FIV-CP group, suggesting an overall increased neuronal injury in this group (data not shown). Thus, dual infection by FIV resulted in a marked reduction in neuronal protein expression in different neuronal subtypes, although synaptic loss was most apparent in the FIV-CP group.

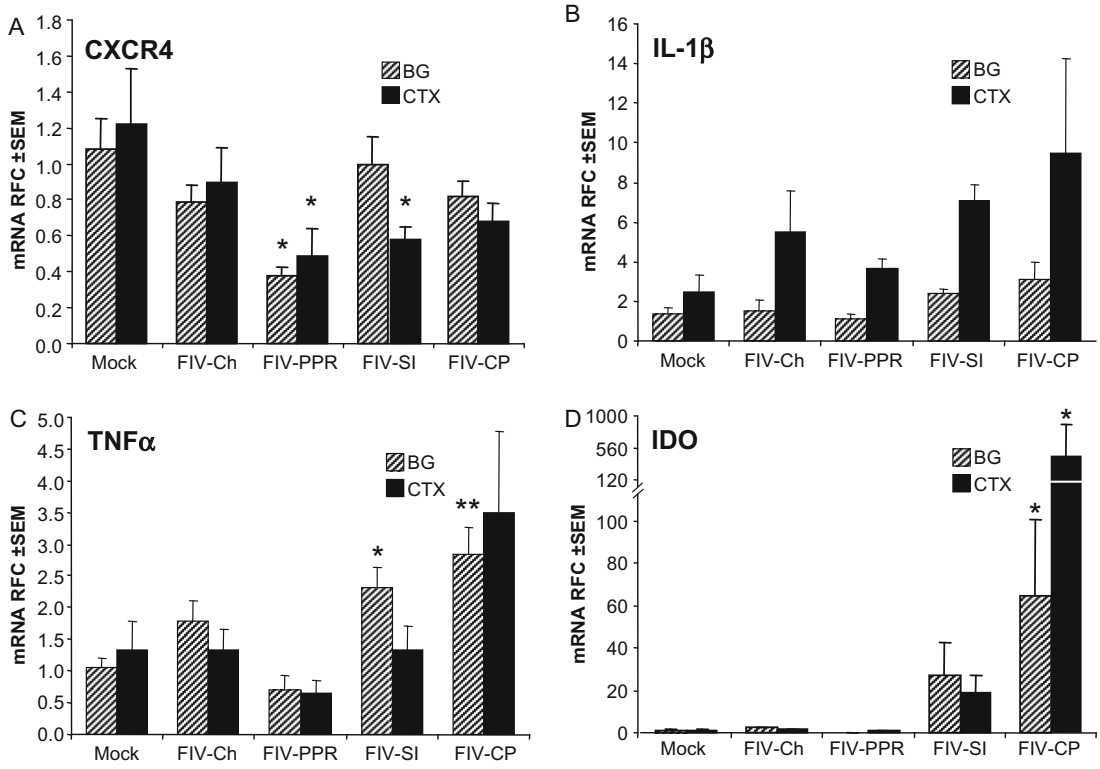

Figure 3 Neuroimmune activation caused by FIV dual infection. (**A**) *CXCR4* expression was reduced in all FIV-infected groups but was most evident in the FIV-PPR group. (**B**) Transcript abundance of host proinflammatory genes was assessed using real-time RT-PCR analysis, revealing up-regulation of *IL-1β* in cortical tissues of brains infected with FIV-Ch, FIV-SI, and FIV-CP. (**C**) *TNF-α* expression was also increased in both dual FIV infection groups. (**D**) Dual FIV infections induced up-regulation of *IDO* in both brain regions, but there was a particularly robust up-regulation of this enzyme in brain cortical regions of cats receiving the FIV-CP. (Data are presented as mean ± SEM; Dunnet's *post hoc* test, $*P < .05$; $**P < .01$; $n \geq 4$ animals per group.)

Dual FIV infection induces in vivo neuroimmune cell activation, neuronal injury, and neurobehavioral deficits

To investigate the neuropathological outcomes of dual FIV infection, and neuroimmune cell activation, we examined the immunoreactivity of select glial activation and neuronal markers in brain sections. Astrocytic (glial fibrillary acidic protein [GFAP]) activation in both FIV-Ch (Figure 5B) and FIV-PPR (data not shown) was evident in infected brains, compared to mock-infected brains (Figure 5A). However, FIV-SI (data not shown) and FIV-CP (Figure 5C) brains showed greater astrocytic activation. Likewise, enhanced microglial activation (ionized calcium-binding adaptor molecule [Iba]-1) was detected in brains infected with FIV-SI (data not shown) and FIV-CP (Figure 5F) compared to brains infected with FIV-Ch (Figure 5E) and FIV-PPR (data not shown), with few Iba-1–immunopositive microglia in mock-infected brains (Figure 5D). NeuN immunoreactivity in cortex disclosed a loss of neuronal nuclei in FIV-infected groups (Figure 5H and I), but these changes were more apparent in the dual-infected groups. Double immunolabeling showed activation of caspase-3 colocalized with the neuronal marker, NeuN, in cortices infected with FIV-Ch (Figure 5H) and FIV-PPR (not shown), compared to mock-infected brains (Figure 5G). Dual infection induced greater cleaved (activated) caspase-3 immunoreactivity in cortical neurons exhibiting dysmorphic changes, including shrinkage in neuronal soma and areas of neuronal loss (Figure 5I). Analysis of neurobehavioral parameters revealed that all FIV-infected groups exhibited

Figure 4 FIV dual infection results in regional neuronal injury. Representative Western blot analyses display immunoreactivities of specific neuronal markers in basal ganglion (figure not shown) and cortex (**A**) from experimental groups. (**B**) There was no difference in synaptophysin immunoreactivity in basal ganglia, unlike the cortex where the dual infections suppressed synaptophysin protein levels, particularly in FIV-CP–infected animals. Immunoreactivity of the cholinergic neuronal, VAChT (**C**), and the GABAergic neuron $GAD_{65/67}$ (**D**) markers did not differ in basal ganglion among groups. In the cortex, on the other hand, dual FIV infections suppressed the expression of these proteins, revealing similar neurotoxic effects in both neuronal populations. Infection with FIV-Ch also suppressed both neuronal proteins in cortex. Semiquantitative, two-color Western blot detection with infrared fluorescence; background-subtracted average intensities of fluorescence units for each band was normalized to the β-actin immunoreactivity and presented as normalized fluorescence ratio (NFR) arbitrary unit (AU). (Data are presented as mean ± SEM; Dunnet *post hoc* test, $*P < .05$; $**P < .01$; $***P < .001$; $n = 4$ animals per group.)

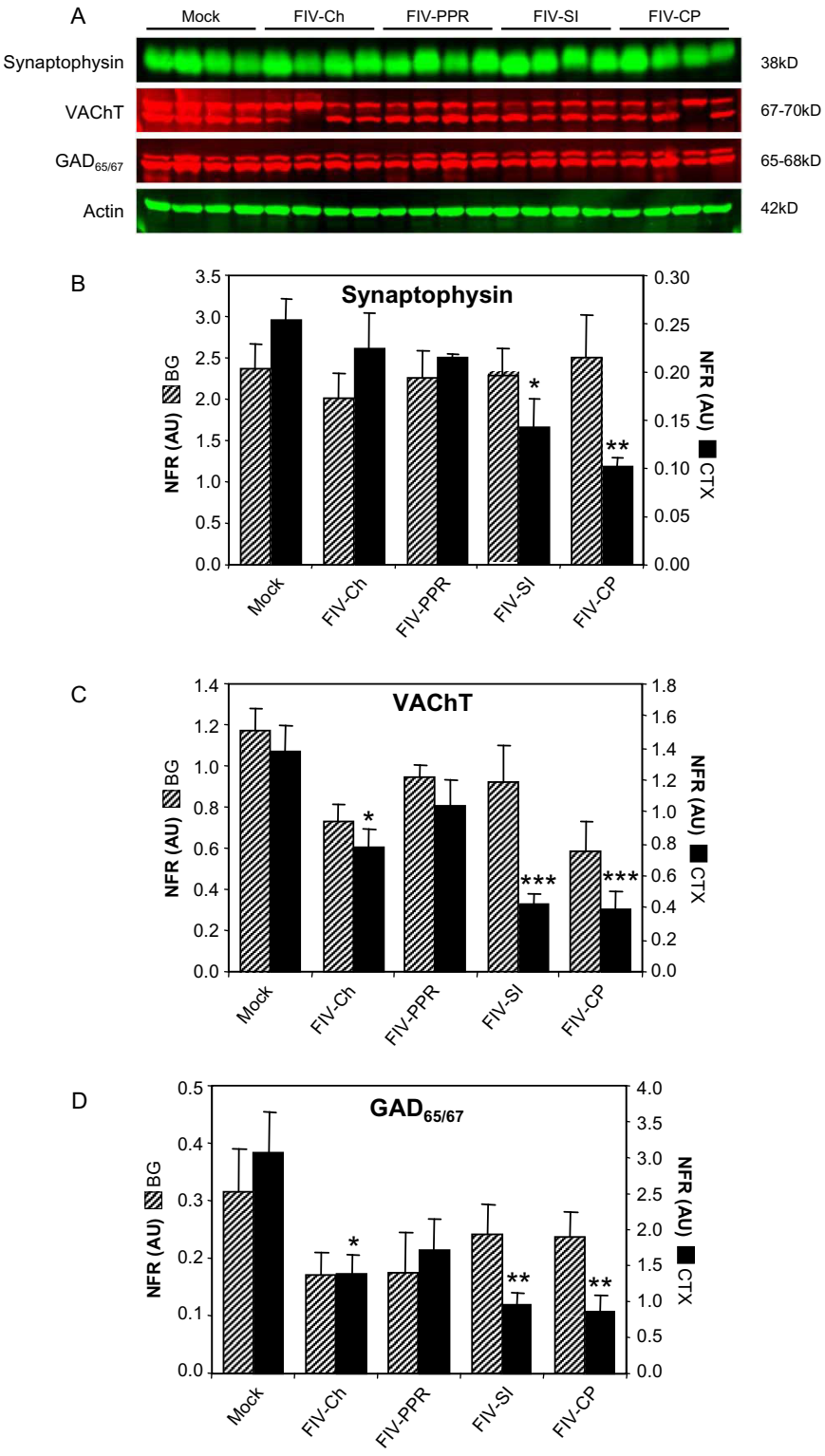

Figure 4 (*Continued*)

worsened in neurodevelopmental performance compared to mock-infected age-matched controls, but these deficits were significantly greater within the group infected with FIV-CP (Figure 5J). Hence, dual FIV infection appeared to have an additive effect on neurovirulence in this lentivirus model that was accompanied by enhanced glial activation and neuronal injury and death.

Discussion

In the present studies, dual FIV infection exhibited detectable levels of both FIV viral strains, FIV-Ch and FIV-PPR, in *ex vivo* and *in vivo* models, which was accompanied by up-regulation of proinflammatory genes and was associated with neurotoxicity. These *ex vivo* effects were more evident in the FIV-SI and FIV-CP models compared to monovirus infections, despite similar levels of viral replication. Although viral burden did not differ among FIV-infection paradigms *in vivo* or *ex vivo*, RFLP-based differentiation of viral strains revealed the presence of both FIV-Ch and FIV-PPR in FIV-CP brains, whereas in the FIV-SI group, only the primary infection (FIV-Ch) was detectable. This finding might reflect an interference mechanism that is established after primary infection contributing to the phenomenon of superinfection resistance, perhaps due to receptor-independent mechanisms. In the absence of differences in viral copy numbers in the CSF, basal ganglia, or cortex and substantial differences in $CD4^+$ T-cell levels among all FIV-infected groups, it is plausible to assume similar neurotropic properties for both viral strains used in this study. Supporting the changes in proinflammatory gene expression during dual lentivirus infections, immunohistochemical analysis revealed more severe astrocytic and microglial activation in dual FIV infections compared to monovirus FIV-Ch– or FIV-PPR–infected groups, with more neuronal injury as evidenced by neuronal caspase-3 immunoreactivity and contemporaneous morphological changes in neurons. Moreover, the present studies suggest that neuronal injury was more evident in the cortex compared to the basal ganglia, involving both cholinergic and GABAergic neuronal populations.

Pathogenic host responses to lentiviral proteins have been demonstrated to have important roles in lentiviral-induced neuroinflammation and subsequent neurotoxicity. Several proinflammatory molecules such as IL-1β and TNF-α are induced in response to infection and inflammation in the brain (Sardar and Reynolds, 1995; Persidsky *et al*, 1997; Nath *et al*, 1999). In the present study, we observed that *IL-1β*, *TNF-α*, and also *IDO* transcript levels were up-regulated in FIV-infected macrophages and brains. Indeed, these changes in host responses were more accentuated in the dual FIV–infected groups (Figure 3). In the current studies, there was substantial variation within individual host responses with groups; this variation (SEM) reflects the use of multiple donors' MDMs from an outlined species, as primary cells' response are known to be diverse due to genetic and environmental factors. Among their proinflammatory effects, the cytokines exert molecular cross-talk, with the expression and activity of indoleamine 2,3-dioxygenase (IDO) in astrocytes and microglia/macrophages. Moreover, IL-1β and TNF-α can act in concert with other immune signaling molecules such as interferon (IFN)-γ to induce IDO expression, accelerating the kynurenine pathway of tryptophan metabolism (Schwarcz and Pellicciari, 2002). This latter pathway produces both neurotoxic (e.g., quinolinic acid) and neuroprotective (e.g., kynurenic acid) metabolites and their ratio might be a good marker of inflammation-induced neurodegeneration. Indeed, the precise mechanism by which IDO is induced by FIV-CP is a topic currently under investigation.

Down-modulation of viral receptors and/or coreceptors on the host cell surface has been postulated to occur due to chronic inflammation and account for interference in retroviral infections (reviewed in Nethe *et al*, 2005). Herein, we observed an *in vivo* reduction in CXCR4 during infection by FIV-PPR and FIV-SI infection of the cortex. This finding suggests that there is variable suppression of viral receptors depending on the individual viral strain or infection paradigm, making cells more or less susceptible to subsequent infection. Exposure to different infectious HIV inocula in high-risk individuals together with high rates of viral production

Figure 5 Dual FIV infections induce neuroimmune cell activation, neuronal apoptosis and neurological disability. (**A**–**C**) Immunohistochemical analysis shows astrocytic activation in FIV-Ch–infected compared to mock-infected brains. However, FIV-CP–infected brains (**C**) had greater astrocytic activation, as evidenced by numerous hypertrophied GFAP-immunopositive astrocytes. (**D**–**F**) Iba-1 immunoreactivity showed enhanced microglial activation in the FIV-CP group (**F**), compared to FIV-Ch–infected brains (**E**), whereas minimal Iba-1–immunopositive microglia were observed in mock-infected cat brains (**D**). Fluorescent staining for Iba-1 (F i) and FIV envelope protein (F ii) revealed the presence of virus in microglial cells as evidenced by double-labeled cells (F iii). (**G**–**I**) Immunohistochemistry disclosed activation of caspase-3 colocalized with the neuronal marker, NeuN, in FIV-Ch–infected cortices. Dual infection induced greater cleaved–caspase-3 immunoreactivity along with morphological changes in cortical neurons, as confirmed by extensive shrinkage in neuronal cell body and areas of neuronal death. **(J)** All FIV-infected groups displayed neurobehavioral deficits as evidenced by higher mean deficit scores (MDS), comprised of multiple tasks, compared to the mock-infected group, although only the FIV-CP group differed from FIV-CH in terms of neurobehavioral performance (original magnification: 200x for **A** to **C** and **G** to **I**, and 2 × 200x for **D** to **F** main panels, 630x for **F** insets, 1000x for **G** and **I** insets). (Data are presented as mean ± SEM; ANOVA, $P < .001$; Tukey-Kramer *post hoc* test, $^*P < .05$; $^{**}P < .01$; $n = 4$ animals per group.)

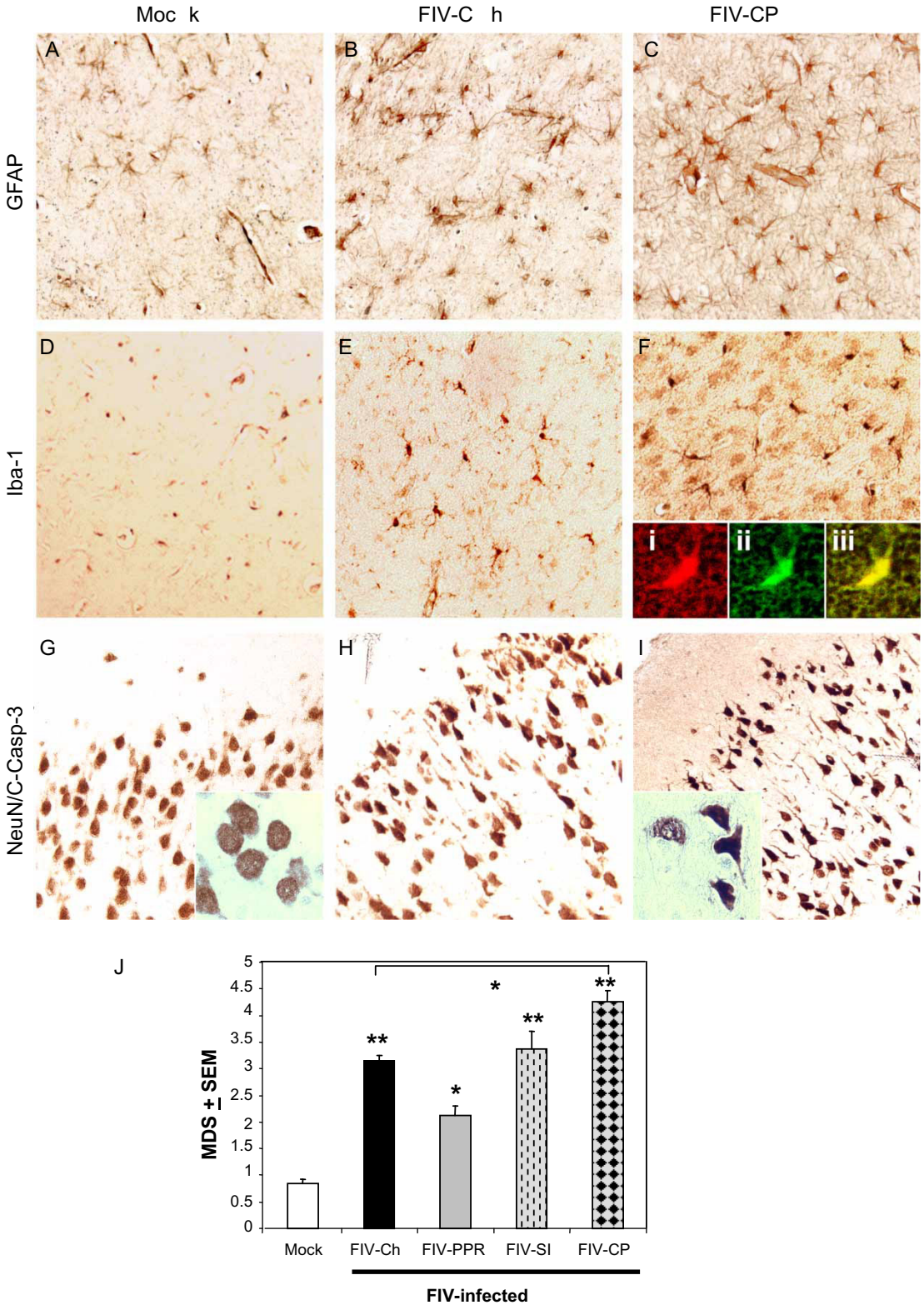

Figure 5 (*Continued*)

in vivo raises the possibility of dual HIV infection with ensuing recombination events, but the impact of relative viral receptor expression or abundance remains unknown. Indeed, several case reports of HIV-1 superinfection (Altfeld *et al*, 2002; Jost *et al*, 2002; Ramos *et al*, 2002; Koelsch *et al*, 2003; Yerly *et al*, 2004; Hu *et al*, 2005; McCutchan *et al*, 2005; Smith *et al*, 2005) and coinfection (Iversen *et al*, 1999; Ramos *et al*, 1999; Becker-Pergola *et al*, 2000; Long *et al*, 2000; Thomson *et al*, 2001) underscore the importance of this phenomenon. There are also reports of recombinant simian immunodeficiency viruses (Jin *et al*, 1994; Georges-Courbot *et al*, 1998), suggesting that recombination is a potential event, although certain genetic barriers exist. A previous study described superinfection of chimpanzees with multiple strains of HIV-1, in which animals protected from superinfection lived longer than did those susceptible to superinfection (Otten *et al*, 1999).

Dual simian immunodeficiency virus (SIV) infection with established neurotropic (macrophage-tropic) and immunosuppressive (lymphotropic) strains results in worsened neurological disease (Zink and Clements, 2002; Weed *et al*, 2003; Zink *et al*, 2006), emphasizing the close coupling of neurological disease and immunosuppression. The present study is the first report describing both *ex vivo* and *in vivo* aspects of dual infection by two neurovirulent lentivirus strains in terms of neurologic disease progression. Although both of the viruses used herein are neuropathogenic, their relative receptor preference remains uncertain and will require further analysis, as will their relative ability to recombine. We were able to detect both viruses used herein in the brain under conditions of coinfection, which emphasizes the persistence of both viruses but future studies are required to further delineate the relative abundance of each strain over time and investigate the time course of recombination events. Our studies also suggest that perhaps HIV-infected patients experiencing infection by different strains of HIV might risk developing more severe immunological and neurological outcomes than individuals who do not encounter a second HIV-1 infection. Increased pathogenicity of dual lentivirus infection could arise because of the generation of recombinant viruses, which have a broader cell tropism or immunosuppressive and neurovirulent properties. However, this is unlikely in the present model given the short duration of infections. As more individuals live longer as a result of more effective antiretroviral treatments, it is likely that higher rates of dual HIV infection will emerge and subsequent recombination will present greater diagnostic challenges, as well as altering drug susceptibility and the progression of immunological and neurological disease outcomes.

Materials and methods

Cell cultures and infectious viruses

Feline peripheral blood mononuclear cells (PBMCs) were isolated and cultured from healthy FIV-seronegative adult animals' blood (Power *et al*, 1998), from which monocyte derived-macrophages (MDMs) were prepared and infected with FIV ($TCID_{50}$ 10^3/ml) (Johnston *et al*, 2002b). The FIV strains used in this study included the primary isolate FIV-PPR (AIDS Research and Reagent Program, NIH, Rockville, MD, USA), and an envelope chimera of V1CSF and Petaluma, FIV-Ch, both titered by limiting dilution (Power *et al*, 1998; Johnston *et al*, 2000, 2002b). FIV copassaged viral stocks were prepared from FIV-PPR and FIV-Ch coinfected healthy PBMCs (at matched input titers) as previously reported (Power *et al*, 1998).

Animals, viral inoculation, and neurobehavioral tests

Adult specific pathogen–free pregnant domestic felines were housed and handled according to Canadian Council on Animal Care guidelines. Neonatal animals were infected intracranially (right parietal lobe) with 100 μl of supernatant from FIV-infected PBMCs (FIV-Ch, FIV-PPR, or mock infected) through a 30-gauge needle, as previously reported (Power *et al*, 1998). For superinfection studies (FIV-SI), animals infected with FIV-Ch strain at postnatal day 1, were subsequently superinfected with FIV-PPR intraperitoneally at week 6 post infection. In coinfection studies, animals were infected at postnatal day 1 with copassaged virus stocks (FIV-CP). Supernatants from uninfected feline PBMCs were used to infect the animals in the control (mock-infected) group. Animals were weaned at 6 weeks of age and monitored until 12 weeks, during which neurodevelopmental performance was assessed weekly, measured as the cumulative mean deficit score (MDS) (van Marle *et al*, 2005). In addition, $CD4^+$ and $CD8^+$ T-cell levels in blood were assessed by flow cytometry (Power *et al*, 1998). After 12 weeks, animals were euthanized, during which brain, cerebrospinal fluid (CSF), and plasma were harvested and stored for further studies.

Measurement of plasma and neural viral load

A real time reverse transcriptase–polymerase chain reaction (RT-PCR) protocol was developed in which the oligonucleotide primers were derived from sequences common to the FIV *pol* gene of multiple strains (PPR, Petaluma), and were used to determine the number of copies of viral RNA in plasma, CSF, and brain tissue (per microgram RNA) (Johnston *et al*, 2000). RNA was extracted from plasma, CSF, and brain, and subsequently cDNA synthesis was performed and viral quantitation was interpreted from a standard curve generated by *in vitro* transcription of the FIV *pol* sequence followed by matched cDNA

synthesis. Viral loads were expressed as viral RNA copies per microgram RNA.

Detection and differentiation of two viral strains
Brain tissue (right frontal lobe) from 12-week control and FIV-infected animals (Johnston *et al*, 2002b) or cultured cells were homogenized and lysed from RNA and corresponding cDNA was prepared (Power *et al*, 2003). Two sets of primers (FIV *pol* sets 1 and 2) containing sequences that were common to the FIV-PPR and FIV-Ch (Petaluma) (Genebank accession numbers: PPR, M36968; Petaluma, M25381) *pol* sequence were designed for gene amplification. The first round of PCR consisted of a 30-cycle amplification using *pol* set 1 to obtain a 214-bp PCR product. Nested PCR consisted of 30-cycle amplification using the *pol* set 2 and 10% of the first-round PCR product as template to obtain a 176-bp PCR product. Set 2 primer sequences were forward primer: 5′-TAG AGA AGC CTG GGA ATC AA-3′ and reverse primer: 5′-CTT TTC CTA GCT TTC TAC CTC C-3′. As there is a single *Dra* I restriction site in FIV-PPR, but not in FIV-Ch, *pol* amplicons from each strain could be distinguished by a *Dra* I–cleaved restriction fragment length polymorphism (RFLP). A nested-PCR protocol was needed to amplify sufficient amount of FIV *pol* for restriction digestion from brain-derived cDNA.

Host gene real-time RT-PCR
PCR primer sequences for host genes *GAPDH* (glyceraldehyde phosphate dehydrogenase), *IL-1β* (interleukin-1β), *TNF-α* (tumor necrosis factor α), and *IDO* (indoleamine 2,3-dioxygenase) expression studies were previously reported (van Marle *et al*, 2005). Semiquantitative analysis of transcript abundance was performed, as previously reported (Power *et al*, 2003), and expressed as relative fold change (RFC) compared to controls.

Neurotoxicity assay
Cholinergic human neuronal (LAN-2) cells were cultured in 96-well plates (Silva *et al*, 2003) and were incubated for 24 h, with supernatants harvested at days 3 and 6 post infection (p.i.) from mock-, FIV-Ch–, FIV-PPR–, and dual-infected feline MDMs. Following fixation and after permeablizing, cells were incubated with LI-COR Odyssey Blocking Buffer before the addition of a mouse monoclonal anti-β-tubulin isotype III (1:800; Sigma, Ontario, Canada) antibody in blocking buffer. Cells were then incubated with fluorescent-labeled secondary antibody goat anti-mouse Alexa Fluor-680 (1:200; Molecular Probes, Eugene, OR, USA) diluted in blocking buffer. After washing, plates were scanned at 700 nm using the Odyssey Infrared Imaging System. Background fluorescence was subtracted for each well before subsequent analysis.

Immunohistochemistry and immunofluorescence staining
Immunohistochemical labeling was performed using 5-μm paraffin-embedded serial brain sections that included basal ganglion (BG) and parietal cortex (CTX) (Tsutsui *et al*, 2004). Sections were incubated overnight at 4°C with antibodies against neuronal nuclei antigen (NeuN; 1:200; Chemicon International, Temecula, CA, USA), cleaved caspase-3 (C-Casp-3; 1:200; Cell Signaling Technology, Danvers, MA, USA), glial fibrillary acidic protein (GFAP; 1:200; Dako, Carpinteria, CA, USA), or ionized calcium-binding adaptor molecule (Iba-1; 1:400; Wako, Tokyo, Japan), in phosphate-buffered saline (PBS) containing 5% normal goat serum and 0.2% Triton X-100. Secondary biotinylated goat antibodies followed by avidin-biotin-peroxidase amplification (Vector Laboratories, Burlingame, CA) and 3,3′-diaminobenzidine tetrachloride staining (Vector Laboratories) were used to detect subsequent immunoreactivity. Secondary alkaline phosphatase–conjugated goat anti-rabbit antibody (1:500; Jackson ImmunoResearch Laboratories, West Grove, PA, USA) followed by Nitro blue tetrazolium chloride/5-Bromo-4-chloro-indolyl phosphate, toluidine salt substrate (Vector Laboratories) were used for double labeling. FIV envelope expression was detected by a monoclonal antibody directed against the FIV envelope surface unit (National Institutes of Health AIDS Research and Reference Reagent Program, catalogue number 4820) and Iba-1, followed by a Cy3- or Alexa 488–conjugated goat anti-mouse secondary antibody (Molecular Probes).

Semiquantitative Western blot analysis
Protein extracts were prepared from feline cortex and basal ganglion tissue with cell lysis buffer, and concentrations were determined by BCA assay (Pierce, Rockford, IL). Fifty microgram of protein was separated by 10% sodium dodecyl sulfate (SDS)-polyacrylamide and transferred onto PVDF membranes, followed by blocking with LI-COR Odyssey Blocking Buffer. Membranes were then probed with monoclonal antisera to neuronal nuclei antigen (NeuN; 1:1000; Chemicon International), or polyclonal antibodies recognizing synaptophysin (Synaptophysin; 1:1000; Santa Cruz Biotechnology, Santa Cruz, CA, USA), vesicular acetylcholine transporter (VAChT; 1:1000; Sigma), glutamate decarboxylase$_{65/67}$ (GAD$_{65/67}$; 1:1000; Chemicon International), or β-actin (sc-1616; 1:1000; Santa Cruz Biotechnology), followed by washing and addition of appropriate fluorescent-labeled Alexa Fluor-680 (1:5000; Molecular Probes) and/or IRDye 800CW (1:1000; Rockland, Gilbertsville, PA, USA) secondary antibodies diluted in blocking buffer supplemented with 0.1% Tween-20 to lower the background. After washing, membranes were scanned simultaneously at 700 and 800 nm using the Odyssey Infrared

Imaging System. Lane-specific background-subtracted average fluorescence intensity of each band was measured and used for subsequent analysis.

Statistical analysis

Statistical analyses were performed by analysis of variance (ANOVA) with Tukey-Kramer or Dunnet multiple-comparison tests as *post hoc* tests, using GraphPad Instat version 3.0 (GraphPad Software). *P* values of less than .05 were considered significant.

Declaration of interest: The authors report no conflicts of interest. The authors alone are responsible for the content and writing of the paper.

References

Altfeld M, Allen TM, Yu, XG, Johnston, MN, Agrawal, D, Korber, BT, Montefiori, DC, O'Connor, DH, Davis, BT, Lee, PK, Maier, EL, Harlow, J, Goulder, PJ, Brander, C, Rosenberg ES, Walker BD (2002). HIV-1 superinfection despite broad CD8+ T-cell responses containing replication of the primary virus. *Nature,* **420:** 434–439.

Andersson, S., Norrgren, H., Dias, F, Biberfeld, G, Albert, J., 1999. Molecular characterization of human immunodeficiency virus (HIV)-1 and -2 in individuals from guinea-bissau with single or dual infections: predominance of a distinct HIV-1 subtype A/G recombinant in West Africa. *Virology.* **262:** 312–320.

Becker-Pergola, G, Mellquist, JL, Guay, L, Mmiro, F, Ndugwa, C, Kataaha, P, Jackson, JB, Eshleman, SH, 2000. Identification of diverse HIV type 1 subtypes and dual HIV type 1 infection in pregnant Ugandan women. *AIDS Res Hum Retroviruses.* **16:** 1099–1104.

Bendinelli, M, Pistello, M, Lombardi, S, Poli, A, Garzelli, C, Matteucci, D, Ceccherini-Nelli, L, Malvaldi, G, Tozzini, F, 1995. Feline immunodeficiency virus: an interesting model for AIDS studies and an important cat pathogen. *Clin Microbiol Rev.* **8:** 87–112.

Blackard, JT, Cohen, DE, Mayer, KH, 2002. Human immunodeficiency virus superinfection and recombination: current state of knowledge and potential clinical consequences. *Clin Infect Dis.* **34:** 1108–1114.

Brumme, ZL, Harrigan, PR, 2006. The impact of human genetic variation on HIV disease in the era of HAART. *AIDS Rev.* **8**: 78–87.

Fang, G, Weiser, B, Kuiken, C, Philpott, SM, Rowland-Jones, S, Plummer, F, Kimani, J, Shi, B, Kaul, R, Bwayo, J, Anzala, O and Burger, H, 2004. Recombination following superinfection by HIV-1. *AIDS.* **18:** 153–159.

Georges-Courbot, MC, Lu, CY, Makuwa, M, Telfer, P, Onanga, R, Dubreuil, G, Chen, Z, Smith, SM, Georges, A, Gao, F, Hahn, BH, Marx, PA, 1998. Natural infection of a household pet red-capped mangabey (Cercocebus torquatus torquatus) with a new simian immunodeficiency virus. *J Virol.* **72**: 600–608.

Hu, DJ, Subbarao, S, Vanichseni, S, Mock, PA, Ramos, A, Nguyen, L, Chaowanachan, T, Griensven, F, Choopanya, K, Mastro, TD, Tappero, JW, 2005. Frequency of HIV-1 dual subtype infections, including intersubtype superinfections, among injection drug users in Bangkok, Thailand. *AIDS.* **19:** 303–308.

Iversen, AK, Learn, GH, Fugger, L, Gerstoft, J, Mullins, JI, Skinhoj, P, 1999. Presence of multiple HIV subtypes and a high frequency of subtype chimeric viruses in heterosexually infected women. *J Acquir Immune Defic Syndr.* **22:** 325–332.

Jin, MJ, Hui, H, Robertson, DL, Muller, MC, Barre-Sinoussi, F, Hirsch, VM, Allan, JS, Shaw, GM, Sharp, PM, Hahn, BH, 1994. Mosaic genome structure of simian immunodeficiency virus from west African green monkeys. *EMBO J.* **13:** 2935–2947.

Johnston, JB, Jiang, Y, van Marle, G, Mayne, MB, Ni, W, Holden, J, McArthur, JC, Power, C, 2000. Lentivirus infection in the brain induces matrix metalloproteinase expression: role of envelope diversity. *J Virol.* **74:** 7211–7220.

Johnston, JB, Silva, C, Hiebert, T, Buist, R, Dawood, MR, Peeling, J, Power, C, 2002a. Neurovirulence depends on virus input titer in brain in feline immunodeficiency virus infection: evidence for activation of innate immunity and neuronal injury. *J NeuroVirol.* **8**: 420–431.

Johnston, JB, Silva, C, Power, C, 2002b. Envelope gene-mediated neurovirulence in feline immunodeficiency virus infection: induction of matrix metalloproteinases and neuronal injury. *J Virol.* **76:** 2622–2633.

Jost, S, Bernard, MC, Kaiser, L, Yerly, S, Hirschel, B, Samri, A, Autran, B, Goh, LE, Perrin, L, 2002. A patient with HIV-1 superinfection. *N Engl J Med.* **347:** 731–736.

Kantor, R, Katzenstein, D, 2004. Drug resistance in non-subtype B HIV-1. *J Clin Virol.* **29:** 152–159.

Kim, JH, McLinden, RJ, Mosca, JD, Burke, DS, Boswell, RN, Birx, DL, Redfield, RR, 1996. Transcriptional effects of superinfection in HIV chronically infected T cells: studies in dually infected clones. *J Acquir Immune Defic Syndr Hum Retrovirol.* **12:** 329–342.

Kim, JH, Mosca, JD, Vahey, MT, McLinden, RJ, Burke, DS, Redfield, RR, 1993. Consequences of human immunodeficiency virus type 1 superinfection of chronically infected cells. *AIDS Res Hum Retroviruses.* **9:** 875–882.

Klausner, RD, Fauci, AS, Corey, L, Nabel, GJ, Gayle, H, Berkley, S, Haynes, BF, Baltimore, D, Collins, C, Douglas, RG, Esparza, J, Francis, DP, Ganguly, NK, Gerberding, JL, Johnston, MI, Kazatchkine, MD, McMichael, AJ, Makgoba, MW, Pantaleo, G, Piot, P, Shao, Y, Tramont, E, Varmus, H, Wasserheit, JN, 2003. Medicine. *The need for a global HIV vaccine enterprise. Science.* **300:** 2036–2039.

Koelsch, KK, Smith, DM, Little, SJ, Ignacio, CC, Macaranas, TR, Brown, AJ, Petropoulos, CJ, Richman, DD, Wong, JK, 2003. Clade B HIV-1 superinfection with wild-type virus after primary infection with drug-resistant clade B virus. *AIDS.* **17:** F11–F16.

Long, EM, Martin HL Jr, Kreiss, JK, Rainwater, SM, Lavreys, L, Jackson, DJ, Rakwar, J, Mandaliya, K, Overbaugh, J, 2000. Gender differences in HIV-1 diversity at time of infection. *Nat Med.* **6:** 71–75.

McCutchan, FE, Hoelscher, M, Tovanabutra, S, Piyasirisilp, S, Sanders-Buell, E, Ramos, G, Jagodzinski, L, Polonis, V, Maboko, L, Mmbando, D, Hoffmann, O, Riedner, G, von Sonnenburg, F, Robb, M, Birx, DL, 2005. In-depth analysis of a heterosexually acquired human immunodeficiency virus type 1 superinfection:

evolution, temporal fluctuation, and intercompartment dynamics from the seronegative window period through 30 months postinfection. *J Virol.* **79:** 11693–11704.

Nath, A, Conant, K, Chen, P, Scott, C, Major, EO, 1999. Transient exposure to HIV-1 Tat protein results in cytokine production in macrophages and astrocytes. A hit and run phenomenon. *J Biol Chem.* **274:** 17098–17102.

Nethe, M, Berkhout, B, van der Kuyl, AC, 2005. Retroviral superinfection resistance. *Retrovirology.* **2:** 52.

Noorbakhsh, F, Tang, Q, Liu, S, Silva, C, van Marle, G, Power, C, 2006. Lentivirus envelope protein exerts differential neuropathogenic effects depending on the site of expression and target cell. *Virology.* **348:** 260–276.

Otten, RA, Ellenberger, DL, Adams, DR, Fridlund, CA, Jackson, E, Pieniazek, D, Rayfield, MA, 1999. Identification of a window period for susceptibility to dual infection with two distinct human immunodeficiency virus type 2 isolates in a Macaca nemestrina (pig-tailed macaque) model. *J Infect Dis.* **180:** 673–684.

Patrick, MK, Johnston, JB, Power, C, 2002. Lentiviral neuropathogenesis: comparative neuroinvasion, neurotropism, neurovirulence, and host neurosusceptibility. *J Virol.* **76:** 7923–7931.

Persidsky, Y, Buttini, M, Limoges, J, Bock, P, Gendelman, HE, 1997. An analysis of HIV-1-associated inflammatory products in brain tissue of humans and SCID mice with HIV-1 encephalitis. *J NeuroVirol.* **3:** 401–416.

Phillips, TR, Prospero-Garcia, O, Puaoi, DL, Lerner, DL, Fox, HS, Olmsted, RA, Bloom, FE, Henriksen, SJ, Elder, JH, 1994. Neurological abnormalities associated with feline immunodeficiency virus infection. *J Gen Virol.* **75(Pt 5):** 979–987.

Power, C, 2001. Retroviral diseases of the nervous system: pathogenic host response or viral gene-mediated neurovirulence? *Trends Neurosci.* **24:** 162–169.

Power, C, Buist, R, Johnston, JB, Del Bigio, MR, Ni, W, Dawood, MR, Peeling, J, 1998. Neurovirulence in feline immunodeficiency virus-infected neonatal cats is viral strain specific and dependent on systemic immune suppression. *J Virol.* **72:** 9109–9115.

Power, C, Henry, S, Del Bigio, MR, Larsen, PH, Corbett, D, Imai, Y, Yong, VW, Peeling, J, 2003. Intracerebral hemorrhage induces macrophage activation and matrix metalloproteinases. *Ann Neurol.* **53:** 731–742.

Power, C, Moench, T, Peeling, J, Kong, PA, Langelier, T, 1997. Feline immunodeficiency virus causes increased glutamate levels and neuronal loss in brain. *Neuroscience.* **77:** 1175–1185.

Prospero-Garcia, O, Huitron-Resendiz, S, Casalman, SC, Sanchez-Alavez, M, Diaz-Ruiz, O, Navarro, L, Lerner, DL, Phillips, TR, Elder, JH, Henriksen, SJ, 1999. Feline immunodeficiency virus envelope protein (FIVgp120) causes electrophysiological alterations in rats. *Brain Res.* **836:** 203–209.

Ramos, A, Hu, DJ, Nguyen, L, Phan, KO, Vanichseni, S, Promadej, N, Choopanya, K, Callahan, M, Young, NL, McNicholl, J, Mastro, TD, Folks, TM, Subbarao, S, 2002. Intersubtype human immunodeficiency virus type 1 superinfection following seroconversion to primary infection in two injection drug users. *J Virol.* **76:** 7444–7452.

Ramos, A, Tanuri, A, Schechter, M, Rayfield, MA, Hu, DJ, Cabral, MC, Bandea, CI, Baggs, J, Pieniazek, D, 1999. Dual and recombinant infections: an integral part of the HIV-1 epidemic in Brazil. *Emerg Infect Dis.* **5:** 65–74.

Salemi, M, Lamers, SL, Yu, S, de Oliveira, T, Fitch, WM, McGrath, MS, 2005. Phylodynamic analysis of human immunodeficiency virus type 1 in distinct brain compartments provides a model for the neuropathogenesis of AIDS. *J Virol.* **79:** 11343–11352.

Sardar, AM, Reynolds, GP, 1995. Frontal cortex indoleamine-2,3-dioxygenase activity is increased in HIV-1-associated dementia. *Neurosci Lett.* **187:** 9–12.

Sarr, AD, Sankale, JL, Gueye-Ndiaye, A, Essex, M, Mboup, S, Kanki, PJ, 2000. Genetic analysis of HIV type 2 in monotypic and dual HIV infections. *AIDS Res Hum Retroviruses.* **16:** 295–298.

Schwarcz, R, Pellicciari, R, 2002. Manipulation of brain kynurenines: glial targets, neuronal effects, and clinical opportunities. *J Pharmacol Exp Ther.* **303:** 1–10.

Silva, C, Zhang, K, Tsutsui, S, Holden, JK, Gill, MJ, Power, C, 2003. Growth hormone prevents human immunodeficiency virus-induced neuronal p53 expression. *Ann Neurol.* **54:** 605–614.

Smit, TK, Brew, BJ, Tourtellotte, W, Morgello, S, Gelman, BB, Saksena, NK, 2004. Independent evolution of human immunodeficiency virus (HIV) drug resistance mutations in diverse areas of the brain in HIV-infected patients, with and without dementia, on antiretroviral treatment. *J Virol.* **78:** 10133–10148.

Smith, DM, Wong, JK, Hightower, GK, Ignacio, CC, Koelsch, KK, Petropoulos, CJ, Richman, DD, Little, SJ, 2005. HIV drug resistance acquired through superinfection. *AIDS.* **19:** 1251–1256.

Takeb, EY, Kusagawa, S, Motomura, K, 2004. Molecular epidemiology of HIV: tracking AIDS pandemic. *Pediatr Int.* **46:** 236–244.

Takehisa, J, Zekeng, L, Miura, T, Ido, E, Yamashita, M, Mboudjeka, I, Gurtler, LG, Hayami, M, Kaptue, L, 1997. Triple HIV-1 infection with group O and Group M of different clades in a single Cameroonian AIDS patient. *J Acquir Immune Defic Syndr Hum Retrovirol.* **14:** 81–82.

Taylor, BS, Sobieszczyk, ME, McCutchan, FE, Hammer, SM, 2008. The challenge of HIV-1 subtype diversity. *N Engl J Med.* **358:** 1590–1602.

Thomson, MM, Delgado, E, Manjon, N, Ocampo, A, Villahermosa, ML, Marino, A, Herrero, I, Cuevas, MT, Vazquez-de Parga, E, Perez-Alvarez, L, Medrano, L, Taboada, JA, Najera, R, 2001. HIV-1 genetic diversity in Galicia Spain: BG intersubtype recombinant viruses circulating among injecting drug users. *AIDS.* **15:** 509–516.

Tsutsui, S, Schnermann, J, Noorbakhsh, F, Henry, S, Yong, VW, Winston, BW, Warren, K, Power, C, 2004. A1 adenosine receptor upregulation and activation attenuates neuroinflammation and demyelination in a model of multiple sclerosis. *J Neurosci.* **24:** 1521–1529.

van Marle, G, Antony, JM, Silva, C, Sullivan, A, Power, C, 2005. Aberrant cortical neurogenesis in a pediatric

neuroAIDS model: neurotrophic effects of growth hormone. *AIDS.* **19:** 1781–1791.

Weed, MR, Hienz, RD, Brady, JV, Adams, RJ, Mankowski, JL, Clements, JE, Zink, MC, 2003. Central nervous system correlates of behavioral deficits following simian immunodeficiency virus infection. *J NeuroVirol.* **9:** 452–464.

Yerly, S, Jost, S, Monnat, M, Telenti, A, Cavassini, M, Chave, JP, Kaiser, L, Burgisser, P, Perrin, L, 2004. HIV-1 co/super-infection in intravenous drug users. *AIDS.* **18:** 1413–1421.

Zhang, K, Hawken, M, Rana, F, Welte, FJ, Gartner, S, Goldsmith, MA, Power, C, 2001. Human immunodeficiency virus type 1 clade A and D neurotropism: molecular evolution, recombination, and coreceptor use. *Virology.* **283:** 19–30.

Zink, MC, Clements, JE, 2002. A novel simian immunodeficiency virus model that provides insight into mechanisms of human immunodeficiency virus central nervous system disease. *J NeuroVirol.* **8 (Suppl 2):** 42–48.

Zink, MC, Laast, VA, Helke, KL, Brice, AK, Barber, SA, Clements, JE, Mankowski, JL, 2006. From mice to macaques—animal models of HIV nervous system disease. *Curr HIV Res.* **4:** 293–305.

This paper was first published online on iFirst on 24 December 2008.